ISSN: 1343-4292
Volume 142, Issue 04, April, 2024

QUALITY CONTROL OF THE AGFA AND KONICA COMPUTED RADIOGRAPHY (CR) SYSTEM

Parkash Pantha[1], Shanta Lall Shrestha[2], Rajendra Prasad Koirala[1*]

Central Department of Physics, Tribhuvan University, Kathmandu, Nepal[1]
Tribhuvan University Teaching Hospital, Kathmandu, Nepal[2]

Corresponding author: 1*

ABSTRACT— Computed radiology (CR) is a widely used digital radiography technique that has largely replaced x-ray film radiography. Some quality parameters must be examined to ensure good contrast in x-ray images at Tribhuvan University Teaching Hospital, Nepal. We estimated and compared three quality parameters of Agfa and Konica photostimulable phosphor imaging systems: limiting spatial resolution, low contrast resolution, and image noise. Limiting spatial resolution and low contrast resolution of PSP system were evaluated by using a DIGRAD (pehamed) test phantom containing resolution test objects. Visual inspection was used to investigate the CR system's limited spatial resolution and low contrast resolution. Image noise of the CR system was evaluated by acquiring images of the low contrast (Plexiglas) test phantom and measuring the standard deviation of pixel values within these specified ROIs with the ImageJ software tool. The limiting spatial resolution was found to be $\geqslant$ 2.1 line pairs per millimeter for both the Agfa and Konica systems. The value of contrast difference was found to be greater than < 1.2% difference, image noise was found to be decreasing with increasing in applied dose, and the noise versus exposure curve was linear. This study shows that the limiting spatial resolution and low contrast resolution observed from the Agfa and Konica computed radiography systems are not in excellent quality at the working place. The image noise of the system is within the tolerable range at higher applied doses and is to be safe for diagnostic purposes.

KEYWORDS: digital, resolution, contrast, noise, photostimulable

1. Introduction

Radiography technique has been successfully transformed over the past few years from film-screen based technology to filmless digital technology. The transition from a film screen environment to a digital is worthwhile to enhance the quality of radiographic images [25]. The radiation dose to the patient can vary during this changeover process. Although the radiation exposure associated with these procedures cannot be completely avoided, it can be minimized. Authorities can take the appropriate actions to guarantee that only secure and correctly placed x-ray equipment are utilized for the proper safety of patients, employees, and the general public [4], [13].

The computed radiography system removes the disadvantages of traditional screen film radiography. Its technology is similar to conventional radiography, except that instead of film, an imaging plate made of photostimulable phosphor is used to create an image [2], [16], [8]. The photostimulable storage phosphors in the CR imaging plate (IP) stores the radiation level received at each point in local electron energies. When the plate is scanned, the scanning laser beam causes electrons to jump to lower energy levels, emitting light that is detected by a photomultiplier tube and converted into an electronic signal. The electronic signal is then converted to discrete (digital) values and loaded into the pixel map of the image

processor. If imaging plates are handled properly, they can theoretically be reused thousands of times [9], [6].

With increased awareness of the need for radiation protection, a shift from the principle of "image quality as good as possible" to "image quality as good as needed" can be seen. Image quality in medical imaging, on the other hand, is a complicated phenomenon. The noise level, spatial resolution, and contrast requirements vary with discipline [11], [27]. There is no specific fix method in digital radiography to maintain constant image quality at different tube potentials in order to calibrate the automatic exposure control (AEC), for the urgent need to develop appropriate practical image quality test methods. To address this issue, medical physics researchers have proposed various types of quality parameters for image quality optimization. The researchers recommend the following parameters: limiting spatial resolution, low contrast resolution, kV*p* performance, uniformity, linearity, image noise, and so on [26], [14], [3], [17].

Spatial resolution is a measurement of how well lines can be resolved in an image. The resolution of an image, rather than the number of pixels in an image, determines its clarity for practical purposes. Several factors contribute to the modulation and loss of the presampled signal in PSP radiography, including physical limits imposed by the composition and thickness of the phosphor plate, the size of the laser spot, PSL temporal lag, and light scattering within the phosphor [1].

The ability to distinguish between intensity in an image is referred to as contrast resolution. In medical imaging, the measure is applied to quantify the quality of acquired images [12], [19]. It is as much dependent on the human observer as on the quality of actual image. Low contrast resolution is used to assess the distinction between two different colors (black and white) in an image. The extent to which two identical objects differ in color is measured by low contrast resolution. Image brightness is to be uniform except where it changes to form an image. Low contrast resolution is affected by a number of factors, including the applied kVp, the amount of scattered radiation, the detector's bit depth, detector efficiency, monitor setting, reading room lighting, and overall system noise [20], [18].

The variation in brightness of the displayed image is referred to as image noise. This variation is typically random and has no discernible pattern. It reduces image quality in many cases, which is especially noticeable when the objects are small. The standard deviation of the pixel value (PVSD) in a fixed small region of the image is used to quantify noise. The noise of the system is investigated using a region of interest (ROI) analysis of the pixel value at various regions of the image. The noise in the system is primarily determined by the x-ray tube dose setting, scattered radiation, detector efficiency, and the reconstruction algorithm. This standard deviation of the pixel value is defined in medical physics as system noise within that specified region [24], [21], [15].

2. Methodology

2.1 X-ray machine

A radiographic image was produced by positioning a portion of the patient in front of an x-ray detector and then illuminating it with a short x-ray pulse. Two machines were used to take radiographs during this work. Figure 1 shows information about the machines, such as operating frequencies and manufacturer.

ISSN: 1343-4292
Volume 142, Issue 04, April, 2024

Machine A
X-ray tube model: - R-20
X-ray tube assembly: - 0.6/1.2PI8DE-85
Serial number: - 3Z7B4A821020
Focal spot size: - 0.6/1.2
Operating frequency: - 50 Hz
Manufacturer: - Shimadzu corporation
Maximum tube voltage: - 150 kV_p

Machine B
X-ray tube number: - 10K586
Unit model: - E7239X
Operating frequency:-50 Hz
Permanent filtration: - 0.9Al/75
Manufacturer: - Toshiba Rotan Ode
Maximum tube voltage: - 125 kV_p

Figure 1: x-rays machines used in experiment.

2.2 Unfors Mult-O-Meter

The Unfors Mult-O-Meter 582L was utilized to measure the dose rate and it is a device for service and quality control (QC) for both conventional and digital radiography. It includes measurements ranging from low input dose rate to high output radiographic exposures (100 nGy - 9999 Gy). It has a wide kV_p range of 45 to 155 kV_p with excellent sensitivity. The meter is simple to operate, with only two buttons to control it: On/Off and Parameter for scrolling the measured values. There is no need for any setup time.

2.3 ImageJ software

ImageJ is a free image processing program written in Java. It is compatible with any computer that has a Java 1.5 or later virtual machine. It can display, edit, analyze, process, save, and print images in 8-bit, 16-bit, and 32-bit resolutions and supports a wide range of image formats, including TIFF, GIF, JPEG, BMP, DICOM, FITS, and "raw". It can compute statistics on the area and pixel value of user-defined selections. It is capable of measuring distances and angles. It is capable of producing density histograms and line profile plots. It can perform standard image processing functions like contrast manipulation, sharpening, smoothing, edge detection, and median filtering [10]. It performs geometric transformations like scaling, rotation, and flipping. Zooming up to 32:1 and down to 1:32 is possible. At any magnification factor, all analysis and processing functions are available. The program supports any number of images at the same time, with the only limitation being available memory [7].

2.4 Test Phantom

The pehamed DIGRAD test phantom was used for quality control of computed radiography. This test phantom incorporates a Huttner line pair phantom at 45o with the horizontal plane. We can test the dynamic range, contrast, exposure homogeneity, and spatial resolution of x- ray systems by using digital image receptors [22]. The test phantom's overall dimensions are 310 mm × 310 mm. Within the detail, a copper plate is embedded in acryl glass plates. Because the acryl glass is white, the light beam can be seen more clearly under spotlighting conditions [23].

3. Results and Discussion

3.1 Measurement of Limiting Spatial Resolution (LSR)

The spatial resolution of the PSP system was measured using the DIGRAD (pehamed) test phantom. The phantom contains a resolution test object angled at 45° with respect to the horizontal plane, similar to the Huttner Line Pair Phantom, and the number of line pairs were evaluated on the working station. Visual inspection was used to investigate the spatial resolution of the CR system. The independent variables were taken three different cassette sizes that were available during the working time. The Unfors Mult-O-Meter was used for measuring the dose applied to the cassette. The signals on the cassette were initially erased in the work station. A focus-detector distance of about 100 cm was set, and collimation was adjusted to collimate the entire cassette to a minimum. The test phantom was placed on the cassette, and a 1 mm copper filter was attached as close to the tube housing as possible. The experiments were carried out at a peak voltage of 70 kV_p, and the correct values of mAs were found to provide a dose of approximately 2.5 µGy. Following the exposure, the cassettes were read with as little image processing as possible and with the gray scale set automatically. To reduce visual error, the line pairs were visually inspected on the working station by three different people. Figure 2 depicts the observed spatial resolution values of the Agfa PSP imaging system and Konica imaging system with respect to the matrix (total number of pixels in an imaging plate) at a fixed value of x-ray tube voltage 70 kV_p.

The resolved lines per mm for a 45o angled test object should be > 1.2/2p, where p is the pixel dimension in mm. The observed value of the limiting spatial resolution at TU Teaching Hospital is less than the recommended value, as shown in Figure 2(a) for the Agfa PSP imaging system and Figure 2(b) for the Konica PSP imaging system. Also, because the pixel size in each cassette is the same, the curve should have been perfectly straight. As a result, the limiting spatial resolution of each cassette is expected to be the same. Furthermore, regardless of cassette size, the spatial resolution for the same matrix should not be affected. Finally, the expected straight and constant limiting spatial resolution curve is obtained.

Though the resolution of the cassette used in the Agfa PSP system was adequate, the digitizer's resolution capacity may be insufficient. In the case of the Konica PSP imaging system, which was used at TU Teaching Hospital, the resolution of the Konica cassette was insufficient when compared to the Agfa PSP system. During the experiment, the collimator in the x-ray machine was not properly opening and closing. Improper collimator operation in an x-ray machine can cause the applied dose to fluctuate, resulting in uneven resolution. Using an old cassette and failing to allow enough time between exposure and reading of the cassette may also contribute to a decrease in the spatial resolution of the PSP imaging system. Furthermore, light amplifying within the phosphor may result to unwanted scattered radiation, causing the resolution of the system to be uneven [5].

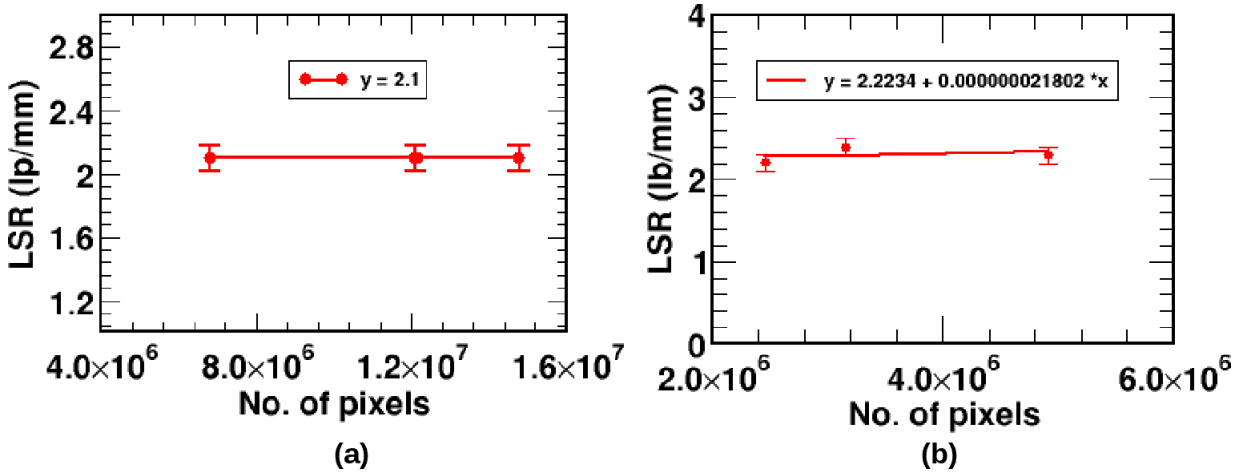

Figure 2: Plot of limiting spatial resolution in (lp/mm) vs total number of pixels in (a) Agfa and (b) Konica

ISSN: 1343-4292
Volume 142, Issue 04, April, 2024

PSP imaging plate, which was exposed to the beam of x-ray containing average applied dose of 2.5 µGy.

3.2 Measurement of Low Contrast Resolution

We investigated low contrast resolution by viewing an image created by the DIGRAD (pehamed) test phantom, which contained various objects with varying contrast values in terms of percentage difference. After exposure, the imaging plate was taken to the work station for visual inspection to determine low contrast. The systems had been calibrated at different kV_p levels. The kV_p was measured and the visual observation was made. To ensure the reproducibility of the kV_p, the dose applied to the PSP system was measured for three consecutive exposures.

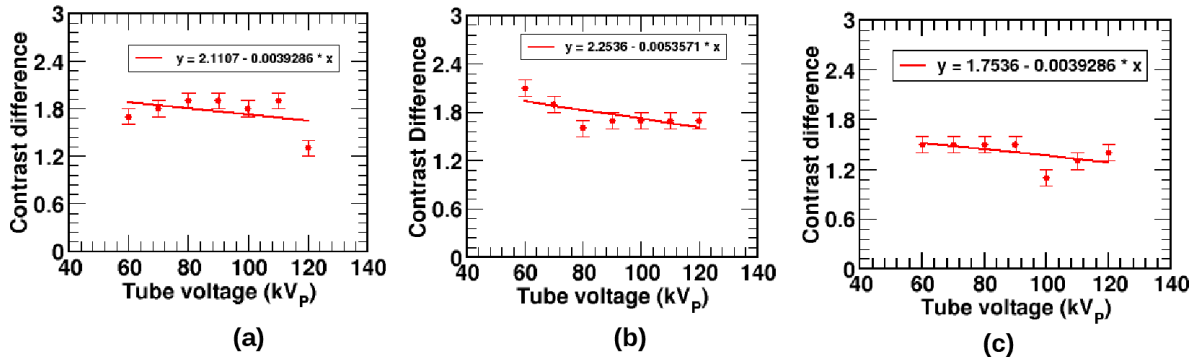

Figure 3: The variation of low contrast resolution of Agfa PSP imaging system for cassette of pixel matrix size (a) 2328 × 2328 i.e., 10" × 12" (b) 3480 × 480 i.e., 14" × 14" (c) 3480 × 4248 i.e., 14" × 17" and pixel size of 100 µm at different values of the tube voltage and at average applied dose of 2.5 µGy.

The focus to detector distance was fixed at 100 cm, and the collimation was set to cover the entire cassette as much as possible. A 1 mm copper filter was attached as close to the tube housing as possible. Various exposures were performed in order to determine the correct mAs value for applying a dose of approximately 2.5 µGy. The test phantom was placed over the cassette, which was on the table, and the collimation was adjusted to cover the entire cassette. There was exposure. This procedure was repeated for three different cassette sizes. The procedure was carried out for kV_p values ranging from 60 to 120. All exposed cassettes were read at the workstation with as little image processing as possible and with the gray scale set automatically. Visual inspection was used to evaluate contrast objects on the workstation, and the value of contrast difference was recorded by three different observers. Figures 3 and 4 show the low contrast resolution of the Agfa PSP imaging system and the Konica imaging system respectively in regards to different values of tube voltage for cassettes with different pixel matrix sizes.

Lower contrast difference indicates better low contrast resolution in computed radiography, and a contrast difference of less than 1.2% is desired for a system. The contrast difference between the Agfa PSP imaging system in Figure 3 and the Konica PSP imaging system in Figure 4 is slightly greater than the recommended value. The graph between the contrast difference and the applied tube voltage is not smooth, but it do decreases slightly as the applied tube voltage increases. Though the applied tube voltage in an x-ray tube increases, the mAs value decreases while the applied dose remains constant. As a result, as the applied kV_p increases, the contrast difference should follow a straight and slightly decreasing curve. Because photons moving towards the imaging plate become more energetic at high voltage and move directly towards the imaging plate. As a result, the radiations are more likely to be scattered, and these scattered radiations contribute significantly to the low contrast difference. We discovered that as the applied tube voltage increases, the contrast difference curve does not decrease significantly, but rather decreases slightly. This is because the test phantom used in this experiment was designed to be slightly thin in order to

reduce the effect of scattered radiation. In addition, a 1 mm thick copper filter was used to reduce the effect of unwanted radiation from the x-ray tube.

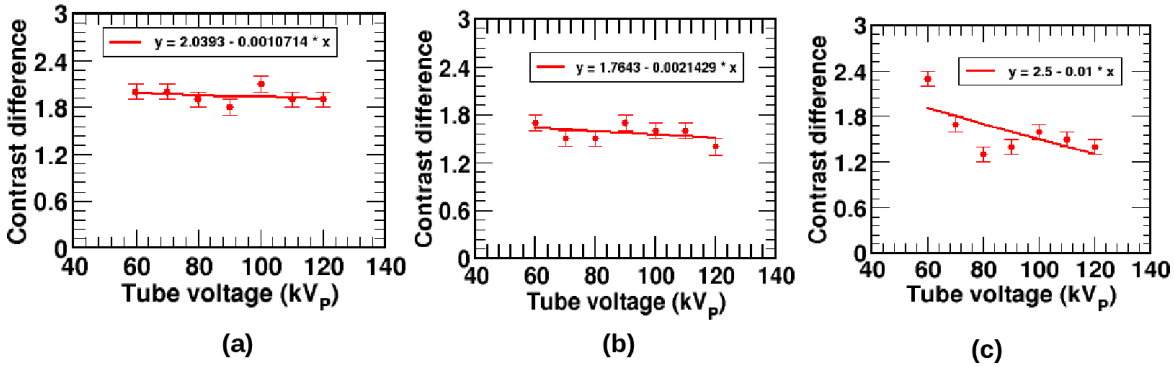

Figure 4: The variation of low contrast resolution of Konica PSP imaging system for cassette of pixel matrix size (a) 1430 × 1722 i.e., 10" × 12" (b) 1572 × 2010 i.e., 11" × 14" (c) 2010 × 2446 i.e., 14" × 17" and pixel size of 175 µm at different values of the tube voltage and at average applied dose of 2.5 µGy.

The low contrast resolution of CR system is also affected by a number of other factors. A slightly higher contrast difference is observed when the system has more system noise. The x-ray machines in the TU Teaching Hospital's x-ray department are long used, and there may be a lack of faithful coherence between the x-ray tube, the cassette used in the experiment, and the digitize. The detector's efficiency was expected to be high, but it was not tested during the experiment. These factors could have contributed to the lower contrast resolution value. The visual inspection method was used to evaluate the low contrast resolution. The gray level, reading distance, monitor setting, and light condition in the reading room could all have influenced the outcome using this method. Reading can also be significantly influenced by the three observers and the background light of the reading room.

3.3 Measurement of Noise

We evaluated the image noise of the CR system by acquiring three images of the low contrast (Plexiglas) test phantom using x-ray beams with energies of 1 µGy, 10 µGy, and 100 µGy at 70 kV_p tube voltage with 1 mm of additional filter attached as close to the tube housing as possible. Three consecutive exposures were made to different cassettes of the same size, with the dose setting remaining constant, i.e., 1 µGy for the first step. Several well-defined locations were specified, and five regions of interest (ROIs) were added to the image at the workstation. Only within the specified regions, these ROIs contain information about pixel value and standard deviation of pixel value. The ImageJ software tool was used to calculate the standard deviation of the pixel value within these specified ROIs. Next, the dose setting is increased from 1 µGy to 10 µGy, and the process is repeated for 100 µGy as well. The logarithm of noise in Agfa and Konica PSP images is plotted against the logarithm of exposure in different regions of the image using ROI analysis. The focus to detector distance (fdd) was 100 cm, and a 1 mm copper filter was used with a fixed tube voltage of 70 kV_p.

The noise of the PSP imaging system is affected by a variety of factors. Scattering radiation contributes significantly to system noise. High energy photons scattered from the test phantom and imaging plate are directed with time delay into the same plate and phantom. These radiations cause a blurred image signal transition onto the imaging plate, which appears on film as noise. The detector's characteristics and efficiency also contribute to noise in the system. In some cases, noise from the laser and photomultiplier can be integrated into the system. An incoherent laser beam can introduce noise into the system. The presence

ISSN: 1343-4292
Volume 142, Issue 04, April, 2024

of noise in the system could also be due to electronic noise.

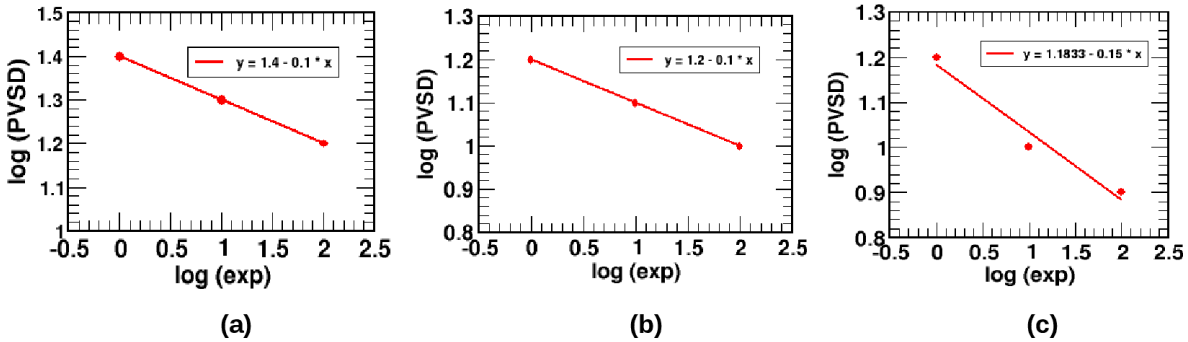

Figure 5: The plot of logarithm of noise of Agfa PSP image with respect to logarithm of the exposure for pixel matrix size of (a) 2328 × 2928 i.e., 10"× 12" (b) 3480 × 3480 i.e., 14" × 14" (c) 3480 × 4248 i.e., 14" × 17" and pixel size of 100 µm at fixed tube voltage 70 kVp and different applied doses.

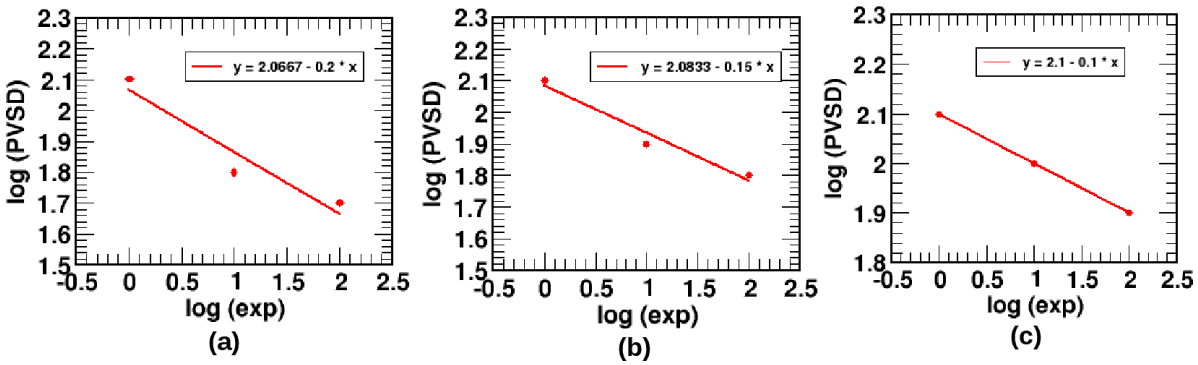

Figure 6: The plot of logarithm of noise of Konica PSP image with respect to logarithm of the exposure for pixel matrix size of (a) 1430 × 722 i.e., 10" × 12" (b) 1572 × 2010 i.e., 11" × 14" (c) 2010 × 2446 i.e., 14" × 17" and pixel size of 175 µm at fixed tube voltage 70 kV_p and different applied doses.

It is recommended that the logarithm of the noise is linearly dependent on the logarithm of the exposure. We investigated the system's noise using ROI analysis of the pixel value at different regions of the image obtained. The logarithm of noise is plotted against the logarithm of exposure, which decreases linearly. In other words, as the energy of the beam of the system (exposure value) increases, so does the noise. Figure 5 depicts the noise variation with exposure for the Agfa PSP imaging system, while Figure 6 depicts the noise variation with exposure for the Konica PSP imaging system. The logarithm of noise in Figure 6 is not perfectly linear, but there is a small deviation in the curve because noise in a system depends on the dose applied. Though the reproducibility of the dose was confirmed by measuring each dose three times, the dose may vary during the final exposure. As a result, variations in applied dose may contribute imperfection of linearity to the curve.

4. Conclusions

We investigated three quality control parameters limiting spatial resolution, low contrast resolution, and image noise, of the computed radiography system at Tribhuvan University Teaching Hospital in Kathmandu, Nepal. The limiting spatial resolution of computed radiography system was ≥ 2.1 lp/mm and was almost identical for different cassettes of the same pixel size. Agfa and Konica Computed Radiography systems were nearly identical. The low contrast difference of CR system was < 2.1% points, and it was slightly greater for the Agfa CR system than the Konica CR system. The CR system's low contrast resolution was found to be increased, i.e., the contrast difference in percentage was observed to decrease

slightly as the applied tube voltage was increased. The image noise of computed radiography system decreased as the applied dose increased. The noise variation with exposure was linear. At low applied dose, the noise for the Agfa computed radiography system was slightly lower than the Konica computed radiography system.

Acknowledgement
We thank to Radiology Department of Tribhuvan University, Teaching Hospital for providing research assistantship as well as research laboratory. Data Availability

All the data that are used to produce the Figures/Tables in this paper are available from the corresponding author in case reproduction is needed.

Conflict of Interest
This is an experimental research work. This manuscript has not been published yet and is not under consideration for publication elsewhere. The work is not intended by any financial or any other personal interest; rather it is sole research motivated. I am ready to take the responsibility regarding any conflict of this work.

5. References

[1] Abadi, E., Segars, W. P., Tsui, B. M., Kinahan, P. E., Bottenus, N., Frangi, A. F., . . . Samei, E. (2020). Virtual clinical trials in medical imaging: a review. Journal of Medical Imaging, 7(4), 042805.

[2] Bushberg, J. T. (2003). The essential physics of medical imaging. Medical Physics, 30(7), 1936.

[3] Cesar, L., Schueler, B., Zink, F., Daly, T., Taubel, J., & Jorgenson, L. (2001). Artefacts found in computed radiography. The British Journal of Radiology, 74(878), 195–202.

[4] Cowen, A., Workman, A., & Price, J. (1993). Physical aspects of photostimulable phosphor computed radiography. The British journal of radiology, 66(784), 332–345.

[5] Fauber, T. L. (2009). Exposure variability and image quality in computed radiography. Radiologic Technology, 80(3), 209–215.

[6] Fujita, H., Ueda, K., Morishita, J., Fujikawa, T., Ohtsuka, A., & Sai, T. (1989). Basic imaging properties of a computed radiographic system with photostimulable phosphors. Medical physics, 16(1), 52–59.

[7] Girish, V., Vijayalakshmi, A., et al. (2004). Affordable image analysis using nih image/imagej. Indian journal of cancer, 41(1), 47.

[8] Hendee, W. R., & Ritenour, E. R. (2003). Medical imaging physics. John Wiley & Sons.

[9] Herrmann, T. L., Fauber, T. L., Gill, J., Hoffman, C., Orth, D. K., Peterson, P. A., . . . Odle, T. G. (2012). Best practices in digital radiography. Radiologic technology, 84(1), 83–89.

[10] Huang, C., Becker, M. F., Keto, J. W., & Kovar, D. (2007). Annealing of nanostructured silver films produced by supersonic deposition of nanoparticles. Journal of Applied Physics, 102(5), 054308.

[11] Khan, F. M. (2010). The physics of radiation therapy. Lippincott Williams & Wilkins.

[12] Landis, J. R., & Koch, G. G. (1977). The measurement of observer agreement for categorical data. biometrics, 159–174.

[13] Lima, R. T., Sousa, D., Paiva, A. M., Palmeira, A., Barbosa, J., Pedro, M., . . . Vasconcelos, M. H. (2016). Modulation of autophagy by a thioxanthone decreases the viability of melanoma cells. Molecules, 21(10), 1343.

[14] Lyra, M. E., Kordolaimi, S. D., Salvara, A.-L. N., et al. (2010). Presentation of digital radiographic systems and the quality control procedures that currently followed by various organizations worldwide. Recent Patents on Medical Imaging, 2(1), 5–21.

[15] Månsson, L. (2000). Methods for the evaluation of image quality: a review. Radiation protection dosimetry, 90(1-2), 89–99.

[16] Marshall, N. (2009). An examination of automatic exposure control regimes for two digital radiography systems. Physics in Medicine & Biology, 54(15), 4645.

[17] Martin, C., Sharp, P., & Sutton, D. (1999). Measurement of image quality in diagnostic radiology. Applied radiation and isotopes, 50(1), 21–38.

[18] Pantha, P., Bhusal, T. P., Shah, B. R., & Koirala, R. P. (2019). Study of natural background radiation in kathmandu valley. BIBECHANA, 16, 187–195.

[19] Parajuli, P., Panday, J. P., Koirala, R. P., & Shah, B. R. (2015). Study of the electromagnetic field radiated from the cell phone towers within kathmandu valley. International Journal of Applied Sciences and Biotechnology, 3(2), 179–187.

[20] Samei, E., & Flynn, M. J. (2003). An experimental comparison of detector performance for direct and indirect digital radiography systems. Medical physics, 30(4), 608–622.

[21] Samei, E., Seibert, J. A., Willis, C. E., Flynn, M. J., Mah, E., & Junck, K. L. (2001). Performance evaluation of computed radiography systems. Medical Physics, 28(3), 361– 371.

[22] Schaff, F., Pollock, J. A., Morgan, K. S., & Kitchen, M. J. (2022). Spectral propagation-based x-ray phase-contrast computed tomography. Journal of Medical Imaging, 9(3), 031506.

[23] Schreiner-Karoussou, A. (2005). Review of image quality standards to control digital x-ray systems. Radiation protection dosimetry, 117(1-3), 23–25.

[24] Svanaes, D. B., Møystad, A., Risnes, S., Larheim, T. A., & Gröndahl, H.-G. (1996). Intraoral storage phosphor radiography for approximal caries detection and effect of image magnification: comparison with conventional radiography. Oral Surgery, Oral Medicine, Oral Pathology, Oral Radiology, and Endodontology, 82(1), 94–100.

[25] Vano, E., Fernández, J. M., Ten, J. I., Prieto, C., Gonzalez, L., Rodriguez, R., & de Las Heras, H.

(2007). Transition from screen-film to digital radiography: evolution of patient radiation doses at projection radiography. Radiology, 243(2), 461–466.

[26] Wilson, A. J., Mann, F., Murphy Jr, W. A., Monsees, B. S., & Linn, M. R. (1991). Photostimulable phosphor digital radiography of the extremities: diagnostic accuracy compared with conventional radiography. AJR. American journal of roentgenology, 157(3), 533–538.

[27] Zhu, T. C., Ahnesjö, A., Lam, K. L., Li, X. A., Ma, C.-M. C., Palta, J. R., . . . Tailor, R. C. (2009). Report of aapm therapy physics committee task group 74: in-air output ratio, for megavoltage photon beams. Medical physics, 36(11), 5261–5291.